JOURNAL OF OPTOELECTRONICS AND ADVANCED MATERIALS Vol. 9, No. 5, May 2007, p. 1322 - 1328

Section 2. Growth and characterization of organic and biological crystals
Invited Paper

Growth and characterization of molecular organic crystals and films

J. FRAXEDAS
Institut de Ciència de Materials de Barcelona (ICMAB-CSIC) Campus de la UAB, E-08193 Bellaterra, Spain

It is reviewed the growth and preparation methods of crystals and thin films of molecular organic materials, which exhibit remarkable physical properties as metallicity, superconductivity and magnetic properties, and the characterization of such physical properties with different experimental techniques.

(Received November 14, 2006; accepted April 12, 2007)

Keywords: Molecular organic materials, Single crystals, Thin films, Physical properties

1. Introduction

The characterization of the intrinsic physical properties of materials strongly relies on the availability of high quality single crystals. The high quality guarantees that the density of defects, that is impurities, dislocations, etc., is sufficiently low. However, the preparation of such ideally perfect crystals is in general a difficult task. Most of the physics studied for molecular organic materials (MOMs) mainly correspond to TTF-TCNQ, BEDT-TTF salts, Bechgaard-Fabre salts, oligomers as α-6T and related compounds as pentacene, because the synthesis of single crystals of extreme perfection is mastered. Fig. 1 shows the schemes, acronyms and reduced names of the most relevant molecules discussed in the text.

When the synthesis of suitable single crystals implies extreme difficulty or when the searched crystallographic phases are metastable, their preparation as thin films becomes the logic alternative. In this case small or large areas of well-selected substrates can be covered with different degrees of homogeneity. However, artefacts associated to the sample morphology, as grain boundaries, grain size, degree of crystallization and orientation, wetting, etc. can mask the intrinsic physical properties. In general many externally accessible variables are involved in the crystallization process (temperature, pressure, molecular flux, distance, time, concentration, solvent, substrate, etc.). These variables, which may be continuous (e. g., temperature) or discrete (e. g., type of solvent), define the parameter hyperspace and the crystallization process of a given crystallographic phase is achieved for a given combination of such variables, defined as a point in the parameter hyperspace. Mathematically this can be regarded as a free energy *G* hypersurface in an *N*-dimensional space, defined by the external variables. Every material has its own free energy hypersurface, which will be characterized by several local minima with different energy barriers. The number of external variables can indeed be very large and depends on the particular growth technique.

Let us next describe shortly the fundamentals of the most common preparation methods, both for the production of single crystals and thin films, illustrated with selected relevant examples. A more detailed discussion can be found in ref. [1].

2. Growth of crystals and films

2.1 Single crystals

Let us start with the *wet preparation methods*. Perhaps the simplest way of obtaining small single crystals, although in an uncontrolled way, is the drop casting technique. This method consists in the deposition of a drop of a saturated solution of a soluble material on a clean substrate and the subsequent evaporation of the solvent. However, when the solvent evaporates in a well-defined way, sufficiently large single crystals can be obtained. This is the case of pentacene, where single crystals are grown from a solution of trichlorobenzene. Violet crystals are obtained by slowly (4 weeks) evaporating the trichlorobenzene at 450 K, under a stream of ultra pure nitrogen gas [2].

Some binary MOMs form very stable phases in solution, which translates in rapid synthetic processes. For instance, TTF-TCNQ can be prepared quite simply as black powder. When highly purified TTF and TCNQ are combined in acetonitrile the 1:1 complex precipitates from the solution. Slowing the crystallization process leads to the formation of single crystals. TTF-TCNQ single crystals with typical dimensions of $2 \times 0.2 \times 0.02$ mm^3 can be grown from solutions of multiply distilled acetonitrile using a U-tube diffusion technique in a glove box filled with argon. High quality crystals are usually obtained after approximately 3 days.

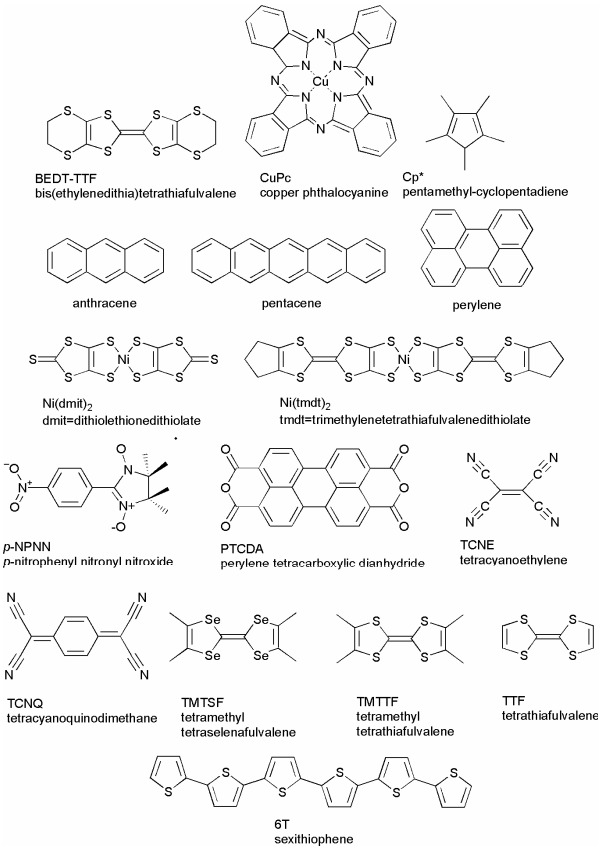

Fig. 1. Schemes, acronyms and reduced names of the most relevant molecules discussed in the text.

The electrocrystallization (EC) technique is a general and versatile synthetic method for the preparation of high-quality single crystals involving molecular ions [3]. The method requires electroactive species (neutral or charged) leading their electrooxidation/reduction to stable radicals. If soluble, the generated radical species may diffuse into solution, but under suitable conditions of concentration, solvent, temperature and current density, they will crystallize on the electrode. The use of a stable and constant direct current source (galvanostatic mode) allows the control of the local concentration of electroactive species and, therefore, the rate of crystal growth. The other parameters involved (concentration, solvent and temperature) essentially control the solubility of the crystalline phase. EC allows high-purity materials to be reproducibly obtained only if all materials and chemicals involved are properly purified. The electrolyte is typically introduced as a tetraalkylammonium or tetra-phenylphosphonium salt to ensure its solubility in the organic solvents necessary to dissolve the donor molecules.

Let us consider the example of the synthesis of $(BEDT\text{-}TTF)_2I_3$ by oxidation of the neutral donor molecule BEDT-TTF. The electrolyte, e. g., TBA I_3, where TBA stands for tetrabutylammonium, would be introduced in both compartments together with the solvent, e. g., acetonitrile, and BEDT-TTF would be introduced in the anode. The salt generated at the anode may crystallize with a 1:1 stoichiometry but frequently the radical cation formed at the electrode associates with one or more neutral donor molecules producing materials with other stoichiometries (1:2, 2:3, etc.) giving rise to mixed valence salts. The extreme quality of these crystals has allowed e. g., the determination of the giant Shubnikov-de Haas oscillations [4]. Modifying the nature of the solvent, the current density and the electrolyte leads to different polymorphs, particularly important for BEDT-TTF -based salts. A last example is $(TMTSF)_2ClO_4$. High-quality crystals can be obtained by oxidation of TMTSF in trichloroethane containing TBA ClO_4. Typical dimensions are $4 \times 0.2 \times 0.2$ mm^3 [5] but centimetre long crystals have been achieved.

When the EC process is forced to occur within two opposite insulating flat substrates (e. g., glass, mica, a thick silicon dioxide layer grown on a silicon substrate, etc.) the technique is termed confined electrocrystallization (CEC) and leads to thin single crystals [6]. This technique can be universally applied, as the parent standard EC technique, to the synthesis of a variety of thin single crystals of conducting and insulating molecular materials. In one of the substrates a metal deposit, e. g., gold, acts as the working electrode. The two substrates are mechanically held together and immersed in the electrolyte solution. In a CEC experiment, there are several prominent differences as compared to standard EC, one of them being the duration of the experiment. While a standard EC experiment can last few days, it takes typically several weeks for CEC experiments. Along the course of an EC experiment in solution, where neutral or charged species are delivered in a steady-state mode to the working electrode, the limiting kinetic step is essentially the electron transfer rate. In a confined environment, the molecular species progress very much slower to the active electrode vicinity. For the growth of radical cation salts it is thus indicated to deposit a thin film of neutral π-donor molecules on the substrate surface (by sublimation under vacuum) prior to the immersion in the electrolyte solution [7,8]. Hence, the effect of slow movement of the electroactive species between the two substrates is compensated by a significant concentration of neutral donor molecules at the anode vicinity. In CEC for a given constant current intensity and with a few μm of gold deposits acting as the anode, the actual current density is typically three orders of magnitude higher than when using a standard platinum wire of 1 mm in diameter. Thus, in order to achieve similar current densities, a set current of 1 μA in the confined experiment configuration should be increased to 1 mA in a classical EC cell.

In order to increase the thin crystal dimensions, a CEC experiment requires to be run at temperatures typically higher than those for the parent EC in solution. However, elevated temperatures favour fully oxidized over mixed valence formulations. This can be exemplified with the superconducting κ-phase, $\kappa\text{-}(BEDT\text{-}TTF)_2Cu(NCS)_2$,which is selectively grown at 298 K, while the insulating phase, $(BEDT\text{-}TTF)Cu_2(NCS)_3$, is obtained instead at 333

K, all other parameters being identical. Thin crystals of κ-(BEDT-TTF)$_2$Cu[(N(CN)$_2$Br], a 2D metal with T_c=11.6 K at ambient pressure, which forms bulk crystals with in standard EC experiments, have also been obtained with CEC displaying the same superconducting transition [8].

Let us now briefly describe *dry preparation methods*. Physical vapour growth in horizontal and vertical systems has been successfully applied to grow millimetre-centimetre sized single crystals of single-component compounds as e. g., α-4T, α-6T, pentacene, anthracene and CuPc [9,10]. A typical apparatus consists of separate source and the deposition tubes within an outer reactor tube. The tubes are wound with resistance wires in order to controllably achieve given temperatures and temperature gradients. Gas inlet and outlet tubes allow the introduction of inert gases as argon, helium and nitrogen, as well as hydrogen. The starting material is usually in the form of purified powder and both the final resulting residual material as well as the crystals can be removed from the tubes after growth. With the help of valves the growth can be performed either in a closed configuration (valves closed) enhancing convection or in an open configuration (valves open), precisely regulating the glass flow.

2.2 Thin films

Let us start again with the *wet preparation methods*. The widely used Langmuir-Blodgett (LB) technique is a way of preparing ultrathin organic films with a controlled layered structure and is based on the assembly of condensed monomolecular films on the surface of water and further transfer to solid surfaces [11,12]. LB films constitute the earliest example of artificial supramolecular assembly, providing a high degree of control over the orientation and placement of molecules in monolayer (ML) and multilayer assemblies that otherwise is hardly obtainable. Furthermore, large uniform substrate areas can be covered with this method. A detailed description of the technique can be found in ref. [13]. Here we give only a glimpse of its fundamentals. A trough is filled with pure water (subphase) and moveable barriers are used to skim the surface of the subphase permitting control of the surface area available to the floating ML. To form a Langmuir ML, the molecule of interest is dissolved in a volatile organic solvent, e. g., $CHCl_3$ or hexane, which will not react with or dissolve into the subphase. Surface active molecules are normally amphiphilic, with separate hydrophilic (-OH, -COOH, -NH_2, etc.) and hydrophobic (-CH_3) groups. A quantity of this solution is placed on the surface of the subphase, and as the solvent evaporates, the surfactant molecules spread. The results are that the hydrophobic tail points towards the air and that the hydrophilic head towards the water surface. Hence the molecules at the interface are anchored, strongly oriented and with no tendency to form a layer more than one molecule thick.

The most common method of LB films transfer is vertical deposition. Either highly hydrophilic or highly hydrophobic substrates are needed. In the conventional LB mode the substrate is dipped vertically through the ML with transfer via the hydrophobic interactions between the alkyl chains and the surface, once the ML has been spread and compressed to the desired transfer pressure. After the ML is stabilized, the substrate is withdrawn from the subphase, and the hydrophilic interactions drive the transfer. Y-type LB films are the most common and are typically the most stable due to the strength of the head-head and tail-tail interactions. Several examples of LB films of molecule-based conductors and magnets have been reported [14,15].

Self-assembled monolayers (SAMs) are ordered molecular assemblies formed by the adsorption of an active surfactant on a solid inorganic surface. As for the LB films case the molecules exhibit two well-differentiated ends groups: head and tail. The adsorbate interacts with the surface through its head group, forming strong covalent bonds (sulphur-gold, carbon-silicon), thus defining robust ML-solid interfaces. The tail chemical function can be selected (methyl, carboxylic acid, amides, etc.) and thus the ML-environment interfaces can be chemically controlled. A detailed discussion of the technique can be found in refs. [16,17]. The preparation of MLs on gold substrates is rather simple [18]. It consists on immersing thin evaporated gold films in dilute solutions. The two external parameters that are varied are the solution concentration (typically few mM) and the immersion time (from few minutes to several hours) in order to control the degree of assembly. The most extensively studied SAMs are alkanethiols on Au(111).

We saw previously that CEC consists in substituting the platinum wire (anode) by a gold film squeezed between two flat insulating substrates. We discuss here the successful example using silicon electrodes as anodes [19]. Intrinsic-type silicon wafers have a sufficiently high conductivity (~10^{-3} Ω^{-1} cm^{-1}) to be used as electrodes. Following this procedure metallic thin films of TTF[Ni(dmit)$_2$]$_2$ and Ni(tmdt)$_2$ have been prepared [20,21].

Let us now discuss on the more relevant *dry preparation methods*. The chemical vapour deposition (CVD) technique can be regarded as the extension of the sublimation method used for the preparation of single crystals discussed before. After introducing the substrates in the reactor, usually made out of glass, and charging the vaporization crucibles with the selected precursor materials, the entire experimental setup is pumped down for several hours (typically overnight) while the mixing zone and the reactor vessel is baked out at the final chosen temperatures. The experiment starts by vaporizing the precursors at low pressures and transported by a carrier gas (typically helium or argon) through heated lines to the mixing zone and then to the deposition zone. What differentiates CVD from other evaporation techniques is that growth units are chemically generated at the mixing zone. The formation of growth units implies either chemical reaction of the precursors, where the resulting final products differ from the precursors (type I), or collective assembling via intermolecular interactions, where the final products and the precursors are identical (type II). [Fe^{+3}(Cp*)$_2$][TCNE]/KBr films correspond to

type I materials and exhibit a Curie temperature T_C of 3.7 K [22]. When purely organic precursors are involved, the CVD technique is termed OCVD, which stands for organic CVD, and corresponds to type II growth. Thin films of TTF-TCNQ grown from its precursors TTF and TCNQ is a good OCVD example [23].

ML control over the growth of organic thin films with extremely high chemical purity and structural precision can be achieved in ultra high vacuum (UHV) by means of organic molecular beam deposition (OMBD), also referred to as Organic Molecular Beam Epitaxy (OMBE). This technique is extremely reliable but complex and expensive. UHV growth has the advantage of providing an atomically clean environment [24]. The study of vapour-deposited organic films has been applied to a large number of molecular systems. However, most of the work has concentrated on the study of the growth and optoelectronic characteristics of planar stacking molecules such as the phthalocyanines and polycyclic aromatic compounds based on naphthalene and perylene. In particular, PTCDA has become extensively studied.

A recently developed alternative to the OMBD technique is the hyperthermal molecular beam deposition (HMBD) method, which has been used to grow e. g., highly ordered pentacene films on metal surfaces [25]. The technique is based on the acceleration of the impinging molecules to a few eV using a seeded supersonic free jet expansion from a molecular beam source in which different inert gases (He, Ar and Kr) can be used as a carrier gas. The fine control of the kinetic energy leads to high quality films. Pentacene films grown by OMBD at room temperature are amorphous while highly ordered films have been grown at low substrate temperatures (200 K) when pentacene molecules with high kinetic energies of a few eV have been deposited on silver substrates [25].

If we allow for a relaxation of the demanding experimental conditions inherent to OMBD by working in a high vacuum environment, instead of UHV, high-quality thin films can also be obtained in a simpler form. We will consider again TTF-TCNQ. High-quality thin TTF-TCNQ films can be obtained by thermal sublimation at ~ 10^{-6} mbar of recrystallized TTF-TCNQ powder. Tapping mode atomic force microscopy (TMAFM) images of such films are shown in Fig. 2. The films consist of highly oriented and strongly textured rectangular-shaped microcrystals, which are oriented with their *a*- and *b*-axis parallel to both the [110] and [-110] substrate directions, respectively, due to the cubic symmetry of the substrates.

The pulsed laser deposition (PLD) technique is widely used for inorganic materials but is becoming increasingly employed for the preparation of thin films of polymers and biomaterials [26]. The working principle is the following. A focused laser pulse passes through an optical window into a vacuum chamber and interacts with a solid surface, the target. The laser pulse is absorbed, and above a given power density, significant material removal occurs in the form of an ejected forward-directed plume. The threshold power density needed to generate such plume depends on the target material, its morphology, the laser pulse wavelength and the laser pulse duration. The organic material targets are usually formed by casting the powder under high mechanical pressure. The use of PLD to deposit organic materials is complicated because of the irreversible induced damage. However, PLD is possible at laser fluences near the ablation thresholds. Examples of thin films grown by PLD are CuPc, Alq_3 and pentacene.

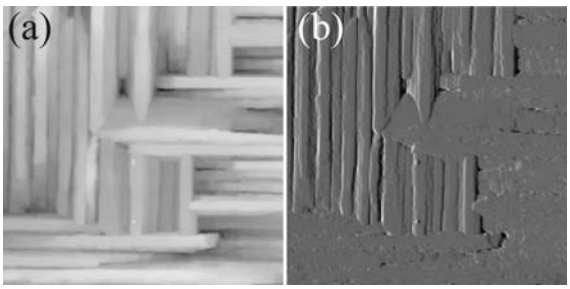

Fig. 2. (a) Topography and (b) amplitude TMAFM images of a thin TTF-TCNQ film (thickness ≈ 1 μm) grown on a KCl(100) substrate. The scale is 5 μm × 5 μm.

In order to minimize the photochemical damage that results from the interaction of the laser light with the organic target, a novel deposition technique, known as matrix-assisted pulsed laser evaporation (MAPLE), has been developed. MAPLE is essentially a variation of the conventional PLD technique and has been successfully used to deposit thin and uniform layers of MOMs, polymers and biomolecules [26]. In MAPLE a frozen matrix consisting of a dilute solution of an organic compound in a relatively volatile solvent is used as the laser target. The photon energy absorbed by the solvent is converted to thermal energy that causes the organic molecules to be heated and the solvent to vaporize. By careful optimization of the MAPLE deposition conditions, this process can occur without any significant chemical decomposition. When a substrate is positioned directly in the path of the plume, a coating starts to form from the evaporated organic molecules, while the volatile solvent molecules, which have very low sticking coefficients, are evacuated by the pump in the deposition chamber.

3. Selected examples

In this section I shall give some examples of MOMs, which I believe are particularly interesting. Let us start by highlighting the role of solvents in the structure-property relationships. Organic solvents not only participate in the synthesis and crystallization of MOMs but they can also form part of new crystallographic phases as guest molecules. These new structures can be regarded as perturbations of the solvent-free phases. Changing the solvent molecule in a given structure may induce dramatic differences in the observed physical properties. A remarkable example is the ternary hybrid β"-(BEDT-TTF)$_4$(guest)[$(H_3O)Fe(C_2O_4)_3$] [27]. If the solvent molecule is C_6H_5CN the material is a superconductor with T_c=8.6 K, while when the guest molecule is C_5H_5N the

resulting material exhibits a metal-insulator transition at 116 K.

The next example concerns polymorphism observed in the Bechgaard-Fabre salts. These salts are usually grown electrochemically on a platinum wire as high quality single crystalline needles by constant low dc oxidation of an organic solution of the corresponding neutral π-donor molecule and the TBA salt of the anion as electrolyte. Under these conditions the triclinic P-1 phase is obtained. However, when synthesized by CEC monoclinic polymorphs are obtained. Let us here discuss on the crystal structure and the corresponding transport properties of μ'-$(TMTTF)_2ReO_4$ [28]. When prepared in the confined geometry single crystals with two different shapes are obtained: rectangular and square platelets. The rectangular crystals are identified as the classical P-1 phase with cell parameters identical to those reported in the literature. On the other hand, the crystal structure of the square shaped crystals is different, as determined by X-ray diffraction. In Fig. 3 the structure for both the classical, $(TMTTF)_2ReO_4$, and the new phase, μ'-$(TMTTF)_2ReO_4$, are illustrated.

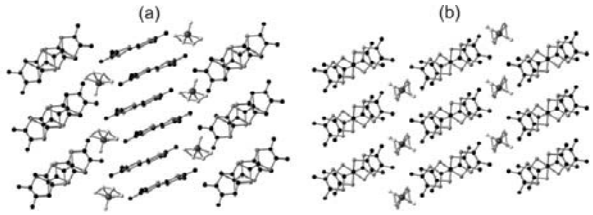

Fig. 3. (a) View of the crystal structure of μ'-$(TMTTF)_2ReO_4$ along the [110] direction (C2/c, a=1.303 nm, b=0.879 nm, c=2.386 nm, β = 97.94°) [28]. (b) Crystal structure of $(TMTTF)_2ReO_4$ at 293 K [29]. C, Re, S and O atoms are represented by black, dark grey, medium grey and light grey balls, respectively. H atoms are omitted for clarity. The two disordered positions of the anions are represented.

In each structure the organic molecules form slabs but in the monoclinic structure each molecular plane is rotated with respect to the next due to a glide plane *c* in the crystal symmetry *C2/c*. The anion is located on a C_2 axis and no longer on an inversion centre. The molecular slabs are quite different between the two structures. The TMTTF columns are more dimerized with a larger longitudinal displacement of the molecule in μ'-$(TMTTF)_2ReO_4$. Overlap between sulphur atoms is less favourable, so interactions between molecules are weaker in μ'-$(TMTTF)_2ReO_4$ than in $(TMTTF)_2ReO_4$. The dimerization should lead to a semiconducting behaviour, which has been indeed observed from single crystal conductivity measurements using the four probe technique [28]. In this case the room temperature conductivity, σ_{RT}, amounts 0.011 Ω^{-1} cm^{-1} and the activation energy, E_a, is 0.17 eV. The triclinic phase is metallic down to 230 K with σ_{RT} =33 Ω^{-1} cm^{-1} [30].

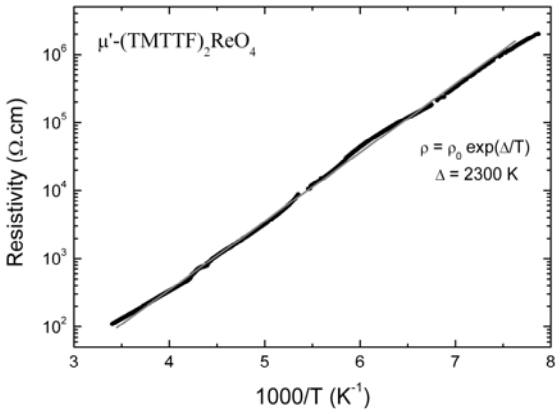

Fig. 4. Resistivity measurements using the four probe technique performed on a μ'-$(TMTTF)_2ReO_4$ thin single crystal. Adapted from [28].

Grain boundaries have, in general, a dominant role on the physical properties of thin films, in particular on the electrical conductivity. Here we shortly highlight two examples of polycrystalline thin films which exhibit truly metallic character, a major achievement when envisioning technological applications. In the vast majority of cases the existence of grain boundaries hinders the metallic behaviour inducing semiconducting-like activated conduction. However, under certain conditions the metallic character can be maintained down to cryogenic temperatures. The first example is $TTF[Ni(dmit)_2]_2$ grown by electrodeposition on silicon wafers [20]. $TTF[Ni(dmit)_2]_2$ single crystals exhibit metallic behaviour down to 3 K, with $\sigma_{RT} \approx 300$ Ω^{-1} cm^{-1} and superconductivity is observed below 1.6 K under application of hydrostatic pressures (above 7 kbar) [31]. The electrodeposited films exhibit metallic character down to ca. 12 K in spite of their polycrystalline morphology with $\sigma_{RT} \approx 10$ Ω^{-1} cm^{-1} [20]. The metallic behaviour evidences that low intergrain conduction energy barriers are achieved, in contrast with most thin films of highly-conducting materials reported to date.

The second example corresponds to the single-component *neutral* molecular material $Ni(tmdt)_2$ grown on silicon substrates. $Ni(tmdt)_2$ is the first synthesized single-component molecular metal, at least down to 0.6 K ($\sigma_{RT} \approx 400$ Ω^{-1} cm^{-1}) [32]. Fig. 5 shows the electrical behavior of the electrodeposited material measured with the standard four-probe method [21]. The figure evidences a clear metallic behavior down to 6 K, except for a small region around 80 K. In this case $\sigma_{RT} \approx 100$ Ω^{-1} cm^{-1}. As expected, because of grain boundary effects, σ_{RT} is clearly lower than the conductivity values found in single crystals.

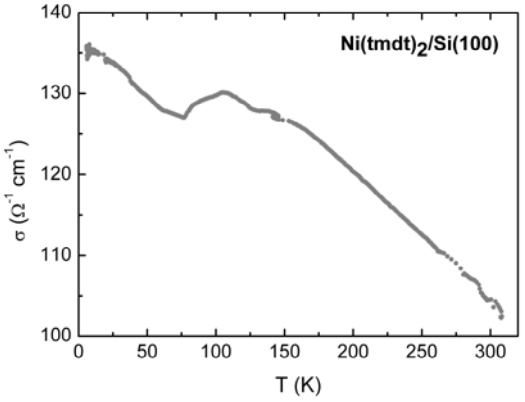

Fig. 5. Temperature dependence of the electrical conductivity of a neutral thin Ni(tmdt)$_2$ film grown on a silicon wafer. The substrate shows a semiconductor behavior with $\sigma_{RT} \approx 10^{-3}$ S cm^{-1}. Adapted from [21].

We can conclude that electrocrystallization is the technique of choice to obtain truly metallic organic thin films of single- and multi-component materials, a necessary step towards the preparation of superconducting films.

Let us conclude this section with the case of the organic radical *p*-NPNN, an amazing material both from its physical properties and crystallization dynamics. Four polymorphs are known for *p*-NPNN: α, β, γ and δ. The thermodynamically most stable β-phase undergoes a ferromagnetic transition (T_c = 0.6 K), while the γ-phase orders antiferromagnetically at T_N = 0.65 K. The metastable α-phase transforms to the β-phase encompassing clearly differentiated structural and morphological changes. However, this transformation is inhibited if the thickness of the films of the initial α-phase lies below a certain critical value (≈ 1 μm) [33]. The mechanism of the α to β solid-solid transformation involves the formation of stable critical nuclei of the β-phase in the initial α-phase. The stability of the α-phase as thin film is induced by residual stress after growth. The nanometer-scale surface morphology of the α-*p*-NPNN thin films is composed by a random distribution of dislocations (spirals) of opposite sign interacting in pairs (Frank-Read mechanism of growth), each spiral emerging from a hollow core. The accumulated stress field after growth induces an increase of the activation energy of formation of critical nuclei of the β-phase in the α-phase matrix. The stability of the α-phase in the form of thin films has allowed the determination of the intrinsic physical properties of this elusive phase [34]. Electron paramagnetic resonance measurements with the static magnetic field applied perpendicular to the substrate plane show that the paramagnetic susceptibility closely follows the Curie-Weiss law, with a Weiss temperature, Θ_W, of -0.3 K, indicating that the net intermolecular interactions are weakly antiferromagnetic. No hint of a transition at low temperature could be observed. These results coincide with those derived from superconducting quantum interference device measurements on a single crystal where $-0.5 < \Theta_W < 0$ [35].

4. Conclusions

In this article I have tried to review the most relevant preparation methods of single crystals and thin films of MOMs and show some examples of their physical properties. It is evident that many examples could have been included but with the excuse of the space limitation I have chosen from a host of available examples those more related to my research. Combining MOMs with biological materials is in its infancy and I believe it will be a successful domain in the years to come.

References

[1] J. Fraxedas, Molecular Organic Materials, From Single Molecules to Crystalline Solids, Cambridge University Press, Cambridge (2006).
[2] C. C. Mattheus, A. B. Dros, J. Baas, G. T. Oostergetel, A Meetsma, J. L. de Boer, T. T. M. Palstra, Synth. Met. **138**, 475 (2003).
[3] P. Batail, K. Boubekeur, M. Fourmigué, J.-C. P. Gabriel, Chem. Mater. **10**, 3005 (1998).
[4] W. Kang, G. Montambaux, J. R. Cooper, D. Jérome, P. Batail, C. Lenoir, Phys. Rev. Lett., 62, 2559 (1989).
[5] K. Bechgaard, K. Carneiro, M. Olsen, F. B. Rasmussen, C. S. Jacobsen, Phys. Rev. Lett. **46**, 852 (1981).
[6] M. Thakur, R. C. Haddon, S. H. Glarum, J. Cryst. Growth **106**, 724 (1990).
[7] Y. F. Miura, S. Ohnishi, M. Hara, H. Sasabe, W. Knoll, Appl. Phys. Lett. **68**, 2447 (1996).
[8] A. Deluzet, S. Perruchas, H. Bengel, P. Batail, S. Molas, J. Fraxedas, Adv. Funct. Mater. **12**, 123 (2002).
[9] Ch. Kloc, P. G. Simpkins, T. Siegrist, R. A. Laudise, J. Cryst. Growth **182**, 416 (1997).
[10] R. A. Laudise, Ch. Kloc, P. G. Simpkins, T. Siegrist, J. Cryst. Growth 187, 449 (1998).
[11] I. Langmuir, J. Am. Chem. Soc. **39**, 1848 (1917).
[12] K. B. Blodgett, J. Am. Chem. Soc. **57**, 1007 (1935).
[13] M. C. Petty, Langmuir-Blodgett films, Cambridge University Press, Cambridge (1996).
[14] M. R. Bryce, M. C. Petty, Nature 374, 771 (1995).
[15] D. R. Talham, Chem. Rev. **104**, 5479 (2004).
[16] A. Ulman, Chem. Rev. **96**, 1533 (1996).
[17] F. Schreiber, J. Phys.: Condens. Matter **16**, R881 (2004).
[18] R. G. Nuzzo, D. L. Allara, J. Am. Chem. Soc. **105**, 4481 (1983).
[19] L. Pilia, I. Malfant, D. de Caro, F. Senocq, A. Zwick, L. Valade, New. J. Chem. **28**, 52 (2004).
[20] D. de Caro, J. Fraxedas, C. Faulmann, I. Malfant, J. Milon, J. F. Lamère, V. Collière, L. Valade, Adv. Mater. **16**, 835 (2004).
[21] I. Malfant, K. Rivasseau, J. Fraxedas, Ch. Faulmann,

D. de Caro, L. Valade, L. Kaboub, J.-M. Fabre, F. Senocq, J. Am. Chem. Soc. **128**, 5612 (2006).
[22] D. de Caro, M. Basso-Bert, J. Sakah, H. Casellas, J. -P. Legros, L. Valade, P. Cassoux, Chem. Mater. **12**, 587 (2000).
[23] A. Figueras, J. Caro, J., Fraxedas, V. Laukhin, Synth. Met. **102**, 1611 (1999).
[24] S. R. Forrest, Chem. Rev. **97**, 1793 (1997).
[25] L. Casalis, M. F. Danisman, B. Nickel, G. Bracco, T. Toccoli, S. Iannotta, G. Scoles, Phys. Rev. Lett., **90**, 206101 (2003).
[26] D. B. Chrisey, A. Piqué, R. A. McGill, J. S. Horwitz, B. R. Ringeisen, D. M. Bubb, P. K. Wu, Chem. Rev. **103**, 553 (2003).
[27] S. S. Turner, P. Day, K. M. Abdul Malik, M. B. Hursthouse, S. J. Teat, E. J. MacLean, L. Martin, S. A. French, Inorg. Chem. **38**, 3543 (1999).
[28] S. Perruchas, J. Fraxedas, E. Canadell, P. Auban-Senzier, P. Batail, Adv. Mater. **17**, 209 (2005).
[29] H. Kobayashi, A. Kobayashi, Y. Sasaki, G. Saito, H. Inokuchi, Bull. Chem. Soc. Jpn. **57**, 2025 (1984).
[30] C. Coulon, P. Delhaes, S. Flandrois, R. Lagnier, E. Bonjour, J.-M. Fabre, J. Physique **43**, 1059 (1982).
[31] L. Brossard, M. Ribault, L. Valade, P. Cassoux, Physica **143B**, 378 (1986).
[32] H. Tanaka, Y. Okano, H. Kobayashi, W. Suzuki, A. Kobayashi, Science **291**, 285 (2001).
[33] J. Fraxedas, J. Caro, J. Santiso, A. Figueras, P. Gorostiza, F. Sanz, Europhys. Lett. **48**, 461 (1999).
[34] S. Molas, C. Coulon, J. Fraxedas, Cryst Eng Comm. **5**, 310 (2003).
[35] M. Tamura, Y. Hosokoshi, D. Shiomi, M. Kinoshita, Y. Nakazawa, M. Ishikawa, H. Sawa, T. Kitazawa, A. Eguchi, Y. Nishio, K. Kajita, J. Phys. Soc. Jpn., **72**, 1735 (2003).

*Corresponding author: fraxedas@icmab.es